JOURNAL OF GEOPHYSICAL RESEARCH, VOL. 104, NO. A2, PAGES 2381–2397, FEBRUARY 1, 1999

Coordinated ISTP satellite and ground observations of morningside *Pc*5 waves

S. Ohtani,[1] G. Rostoker,[2] K. Takahashi,[3] V. Angelopoulos,[4] M. Nakamura,[5]
C. Waters,[6] H. Singer,[7] S. Kokubun,[3] K. Tsuruda,[8] W. J. Hughes,[9] T. A. Potemra,[1,10]
L. J. Zanetti,[1] J. B. Gary,[1] A. T. Y. Lui,[1] and D. J. Williams[1]

Abstract. This paper reports the result of a coordinated data analysis of a morningside *Pc*5 event observed at different altitudes in the magnetosphere and also on the ground. The event took place during 1400–1500 UT of April 29, 1993. The Geotail satellite was located in the boundary region and observed a 5-min quasi-periodic magnetic oscillation. The oscillation was mostly transverse to the background magnetic field. A 90° phase lag between the magnetic field and electric field variations was not clear, suggesting that the oscillation was not a standing wave and that Geotail was located in or close to the excitation region. The plasma flow vector rotated clockwise on the equatorial plane viewed from the north as expected for a magnetospheric surface wave on the morningside. At geosynchronous altitude, the GOES satellites also observed a 5-min magnetic oscillation but with a significantly smaller amplitude than at the Geotail position. Five-minute magnetic oscillations were also detected at Canadian Auroral Network for the OPEN Program Unified Study (CANOPUS) and Magnetometer Array for Cusp and Cleft Studies (MACCS) ground stations in the same local time sector as the satellites, even equatorward of a region 2 field-aligned current observed by the Freja magnetometer data. From the phase analysis of ground signatures, the wave is inferred to propagate westward (antisunward) at a velocity of 18° in longitude per minute. The propagation speed mapped to the equator, 400 km/s, is in the range of the expected flow speed of the magnetosheath. It is inferred that in the present event, the Kelvin-Helmholtz instability at the magnetopause, rather than at the inner edge of the boundary layer, excited an oscillation at the single frequency in a large area from the boundary region to deep inside the magnetosphere.

1. Introduction

Low-frequency magnetic pulsations with a period of 150 to 600 s (the *Pc*5 frequency range) have been investigated both experimentally and theoretically [see, e.g., *Samson*, 1991; *Anderson*, 1994]. It has been generally accepted that the characteristics of *Pc*5 pulsations are different in the morning and evening sectors [*Takahashi and McPherron*, 1984; *Kokubun*, 1985; *Kokubun et al.*, 1989; *Anderson et al.*, 1990]. Pulsations in the morning sector are most likely excited externally, whereas those in the evening sector are often related to an internal process of the magnetosphere.

The frequent occurrence of *Pc*5 waves in the morning sector has been established by observations at various altitudes in the magnetosphere and on the ground. Repeated magnetopause crossings with periods in the *Pc*5 range were found at a very early stage of spacecraft observation [*Aubry et al.*, 1971]. After the low-latitude boundary layer (LLBL) was found [*Eastman et al.*, 1976; *Eastman and Hones*, 1979], low-frequency pulsations near the magnetopause were examined in terms of the structure of the boundary layer [e.g., *Sckopke et al.*, 1981; *Couzens et al.*, 1985; *Takahashi et al.*, 1991; *Sarafopoulos*, 1993; *Chen et al.*, 1993; *Nakamura et al.*, 1994; *Seon et al.*, 1995]. Those waves were found to propagate antisunward at a velocity of 300 to 400 km/s [*Lepping and Burlaga*, 1979; *Chen et al.*, 1993].

Inside the magnetosphere, morningside magnetic pulsations are usually transverse and are polarized in the azimuthal direction [*Takahashi and McPherron*, 1984; *Kokubun*, 1985; *Kokubun et al.*, 1989; *Anderson et al.*, 1990]. Satellite observations indicate that the dominant standing structure of morningside *Pc*5 waves is the fundamental mode [*Singer and Kivelson*, 1979; *Cahill et al.*, 1986; *Potemra et al.*, 1989; *Mitchell et al.*, 1990; *Anderson et al.*, 1990], although the coexistence of higher harmonics is often observed [e.g., *Takahashi and McPherron*, 1982; *Takahashi et al.*, 1984].

The antisunward propagation [*Olson and Rostoker*, 1978] and the fundamental standing structure [*Kokubun et al.*, 1976] were also found for morningside *Pc*5 pulsations observed on the ground. The

[1]Applied Physics Laboratory, The Johns Hopkins University, Laurel, Maryland.
[2]Department of Physics, University of Alberta, Edmonton, Canada.
[3]Solar-Terrestrial Environment Laboratory, Nagoya University, Toyokawa, Japan.
[4]Space Science Laboratory, University of California, Berkeley.
[5]Department of Earth and Planetary Physics, University of Tokyo, Japan.
[6]Department of Physics, University of New Castle, Callaghan, Australia.
[7]R/E/SE NOAA, Boulder, Colorado.
[8]Institute of Space and Astronautical Science, Sagamihara, Japan.
[9]Department of Astronomy, Boston University, Boston, Massachusetts.
[10]Deceased April 3, 1998.

Paper number 1998JA900037.
0148-0227/99/1998JA900037$09.00

latitudinal profile of the ground wave amplitude often has a peak, and the polarization of waves is opposite on the different sides of the amplitude peak [*Samson et al.*, 1971]. The polarization is clockwise on the poleward side of the reversal, whereas it is counterclockwise on the equatorward side. The collocation of the polarization reversal and the amplitude peak was also found for ionospheric electric field variations [*Greenwald and Walker*, 1980]. Such latitudinal dependence is well explained in terms of the field line resonance model [*Tamao*, 1966; *Southwood*, 1974; *Chen and Hasegawa*, 1974].

The Kelvin-Helmholtz (K-H) instability at or near the outer boundary of the magnetosphere has been suggested as the source of morningside *Pc*5 waves. The observed antisunward propagation of waves is consistent with this idea. Furthermore, it is known that high-speed solar wind flows are favorable for the occurrence of waves observed near the magnetopause [*Seon et al.*, 1995], inside the magnetosphere [*Kokubun et al.*, 1989], and on the ground [*Wolfe et al.*, 1980]. A close association between ground low-frequency fluctuations and a convection reversal has been reported [*Clauer et al.*, 1997], suggesting that the flow shear is important for the wave generation.

To understand the excitation mechanism and spatial structure of morningside *Pc*5 waves, it is essential to examine in situ observations of the wave excitation in association with signatures inside the magnetosphere or on the ground. However, there are very few such studies. The only example that we are aware of was reported by *Kivelson and Chen* [1995], who reported an event in which the ground magnetic field fluctuated at the same frequency as the oscillatory motion of the magnetopause.

In the present study, we examine an event that took place on April 29, 1993. In this event, the Geotail satellite was located at the morningside flank of the magnetosphere and observed *Pc*5 waves with a period of 5 min. Magnetic pulsations with the same oscillation period were also observed at geosynchronous altitude and on the ground. The data sets are examined in section 2. In section 3, we compare the results of the present study with previous results and discuss the excitation mechanism of morningside *Pc*5 waves. Section 4 is a summary.

2. Observations

2.1. Coordinates of Satellites and Ground Stations

Figure 1a shows the locations of the Geotail, GOES 6, and GOES 7 geostationary satellites for the interval of 1400 to 1500 UT, projected onto the *x*-*y* plane in geocentric solar magnetospheric (GSM) coordinates. Geotail was inbound in the early morning sector; the satellite moved from (–6.7, –13.9, –2.4) to (–5.3, –13.3, –2.8) R_E in GSM during this 1-hour interval. The two GOES satellites were located in the morning sector; the local time of GOES 6 was 1.9 hours earlier than that of GOES 7. The solid lines represent the expected positions of the bowshock and the magnetopause, calculated by the empirical formulae reported by *Fairfield* [1971] and *Roelof and Sibeck* [1993], respectively, for a typical solar wind condition with an interplanetary magnetic field (IMF) B_Z component of 0 nT and a solar wind dynamic pressure of 2 nPa; no solar wind data are available for this event. For the variability of the magnetopause shape for different IMF conditions see *Roelof and Sibeck* [1993, Figure 9].

Figure 1b shows the locations of ground magnetometer stations along with the footpoints of Geotail, GOES 6, and GOES 7 in the frame of invariant latitude versus magnetic longitude. Magnetic local times (MLTs), which were calculated based on the Polar Anglo-American Conjugate Experiment (PACE) model field [*Baker and Wing*, 1989], correspond to 1430 UT. Also shown by the solid line is the ionospheric projection of the trajectory of the Freja satellite; the satellite's location is marked every minute. The footpoint of Geotail was calculated every 12 min for the Tsyganenko 89, the Mead and Fairfield, and the Tsyganenko 87 models; the results are presented by the different marks in this order of the model fields from poleward to equatorward in the figure. The calculation was done with the Locator software available at the NASA Satellite Situation Center for $Kp = 3$, the actual Kp index for the present interval. The footpoint was moving westward (antisunward) because of the Earth's revolution. Although the footpoints of the two GOES satellites were also calculated for the different model fields, the result is represented by a single point for each satellite because it does not significantly depend on the model fields or universal times. We emphasize that these footpoints should be regarded only as suggestive, especially for Geotail, which was located close to the magnetopause.

For the present event, magnetometer data from Canadian Auroral Network for the OPEN Program Unified Study (CANOPUS) and Magnetometer Array for Cusp and Cleft Studies (MACCS) stations (though not from all stations) are available. The locations of these stations are listed in Table 1 and also shown in Figure 1b. The footpoints of GOES 6 and 7 are on the opposite sides of the meridional chain (RAN-PIN) and are in the same latitudinal range as the east-west chain (GIL to SMI).

Unfortunately, no solar wind data are available for this event. Nightside auroral zone stations, such as Tixie (invariant latitude = 65.2°, MLT = 22.5 at 1430 UT) or Chokurdakh (invariant latitude = 64.3°, MLT = 23.5), did not observe any clear substorm activities until a modest amplitude (≈ 250 nT) negative bay started at 1530 UT (K. Yumoto, private communication, 1998), suggesting that the IMF was not strongly southward during the event. Particle precipitation data acquired by the DMSP satellites suggest that the IMF Z component was northward during the first half of the 1-hour interval (1400–1500 UT) but was more likely southward during the second half (P. T. Newell, private communication, 1998).

2.2. Geotail Signatures

Figure 2 shows the Geotail magnetic field (MGF) [*Kokubun et al.*, 1994a] and energetic particle (EPIC) data [*Williams et al.*, 1994] during the interval of 1300 to 1600 UT. Figure 2a plots the GSM z magnetic field component and the total field strength. The similarity of the two plots indicates that the magnetic field was almost northward. The stable magnetic orientation is also suggested by the small ratio of the standard deviation to the total field strength, which is plotted in Figure 2b. Figures 2c and 2d present the azimuthally sectored flux of protons in the energy range of 9.27 to 215 keV and the energy-time diagram of protons in the grayscale, respectively. There is no clear asymmetry between the sunward and antisunward fluxes, indicating that the satellite was not in the magnetosheath but in the magnetosphere [*Williams et al.*, 1985]; this will be confirmed later by the stagnant nature of plasma convection (Figure 3a). The tendency of the energetic particle flux to increase until 1445 UT (Figure 2d) suggests the inward movement of the satellite relative to the magnetopause. We also infer from the northward magnetic orientation that the satellite was close to the equatorial plane.

Figure 3 combines the Geotail magnetic field and electric field data [*Tsuruda et al.*, 1994]; unfortunately, no measurement from the Low Energy Plasma experiment is available for this event. Here we used 45-s binomial sliding averages based on 3-s data. The

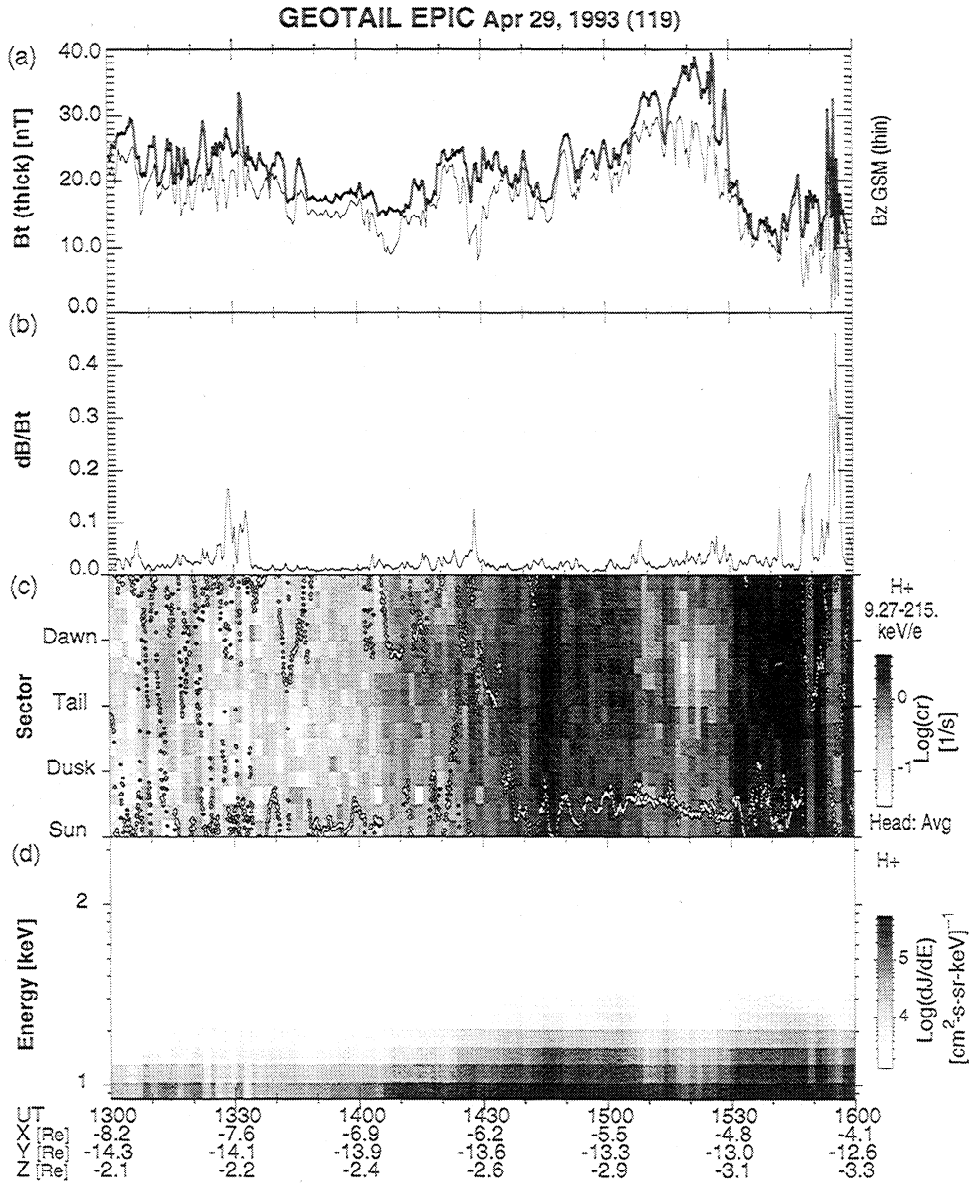

Figure 2. Geotail magnetic field and energetic particle data. (a) 96-s averages of the GSM z magnetic field component (thin line) and the total field strength (thick line). (b) The ratio of the standard deviation of magnetic fluctuations to the background magnetic field strength. (c) The sectored flux data of protons in the energy range of 9.27 to 215 keV. (d) The differential number flux of protons.

magnetic field component (i.e., E_Y for B_X, and E_X for B_Y) is plotted, whereas the same component is plotted in Figure 3d. The scale of the electric field data is given on the right-hand side of each panel, and it is inverted for E_Y so that a systematic phase difference between magnetic field and electric field oscillations would appear in the same sense in the second and third panels.

The B_Y plot shows quasi-periodic oscillations with an approximate period of 5 min. The peak-to-peak amplitude of the oscillations was about 10 nT. Although the B_X plot also shows large fluctuations, the characteristic period of fluctuations seems to be shorter than 5 min, which will be confirmed by the power spectrum. Something transient happened around 1430 UT, when B_X decreased coincidentally with a positive peak of E_X.

Although the 5-min oscillation was continuous in the y magnetic component, the characteristics of the oscillation changed during the interval. For the first several cycles, the 5-min oscillation was confined in B_Y except for some possibly associated variations in B_X, and B_Z did not show any evident periodic variation. In other words, the oscillation was transverse to the background field. For the later interval, the oscillation was compressional as well as transverse, as indicated most manifestly by the three-cycle variation of B_Y and B_Z during 1450 to 1505 UT. This change of the characteristics of the 5-min oscillation might be related to the transient phenomenon around 1430 UT, which was detected globally, as will be shown later.

Figure 4 compares the power spectral densities (PSDs) of the three magnetic components and the total field strength for the interval of 1405 to 1456 UT. Each magnetic component was linearly detrended before the analysis, and the plots of the PSDs of B_X and B_Z are offset as denoted in Figure 4. The 5-min B_Y oscillation is clearly indicated by the peak at 3.3 mHz. The PSD of B_X has a peak at a higher frequency (5.9 mHz), which is consistent

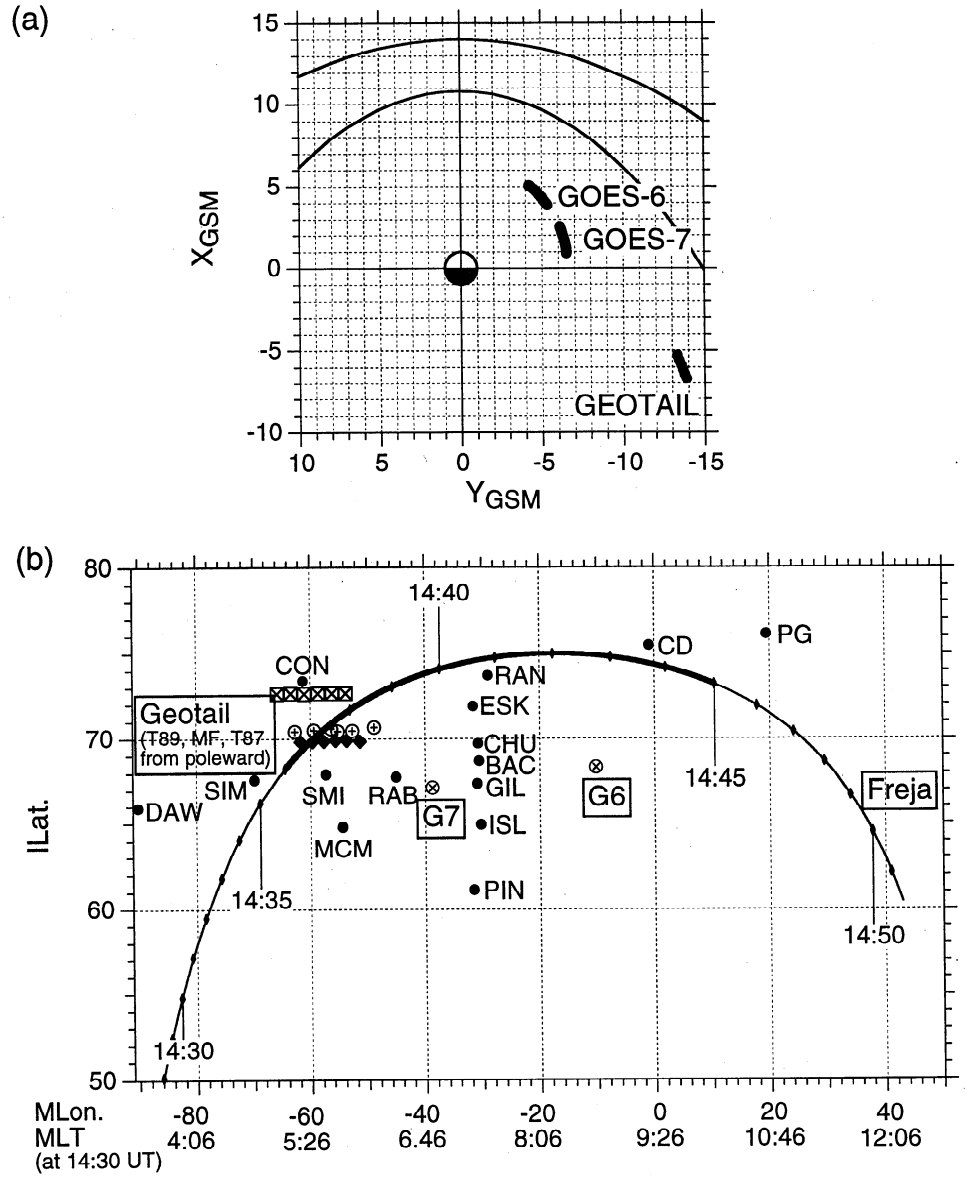

Figure 1. (a) The locations of the Geotail, GOES 6, and GOES 7 satellites during 1400 to 1500 UT of April 29, 1993, projected on the GSM x–y plane. (b) The locations of ground stations (listed in Table 1) in the frame of invariant latitude versus magnetic longitude, along with the footpoints of the satellites. Also plotted is the trajectory of the Freja satellite, with a mark every minute.

Table 1. Locations of Ground Stations

Station	Geographic		PACE Geomagnetic	
	Lat.	Long.	Lat.	Long.
PG (Pangnirtung)	66.1	294.2	76.1	19.6
CD (Cape Dorset)	64.2	283.4	75.5	–0.9
RAN (Rankin inlet)	62.8	267.9	73.7	331.0
ESK (Eskimo Point)	61.1	266.0	71.9	328.4
CHU (Fort Churchill)	58.8	265.9	69.7	329.2
BAC (Back)	57.7	265.8	68.7	329.4
GIL (Gillam)	56.4	265.4	67.4	329.1
ISL (Island Lake)	53.9	265.3	64.9	329.7
PIN (Pinawa)	50.2	264.0	61.2	328.4
RAB (Rabbit Lake)	58.2	256.3	67.8	315.0
SMI (Fort Smith)	60.0	248.1	67.9	302.7
SIM (Fort Simpson)	61.8	238.8	67.6	290.1
CON (Contwoyto Lake)	65.8	248.8	73.4	298.8

electric field vector was determined from the measurements of two spin-plane components, which are parallel to the ecliptic plane, by assuming that there is no field-aligned component.

Figure 3a plots the x component of the electric field drift, V_X. At the beginning of the interval, V_X was fluctuating but was biased negatively by a few tens of km/s. That is, the plasma was convected antisunward at a velocity much slower than the typical magnetosheath flow. We conclude that Geotail was initially located in the boundary layer. However, such a negative bias of V_X was not clear for the later period, implying that the satellite was moving inward. For the later interval, Geotail was likely to be in the stagnation region of the boundary layer [*Williams et al.*, 1985; *Traver et al.*, 1991] or in the plasma sheet.

The other three panels of Figure 3 (b, c, and d) plot the Geotail magnetometer data, B_X, B_Y, and B_Z, respectively, in GSM coordinates. The dashed lines are electric field measurements. In Figures 3b and c, the electric field component perpendicular to the plotted

with our visual examination of Figure 3. Although the PSD of B_Z also has a peak at 3.3 mHz, its amplitude is smaller than that of B_Y by an order of magnitude. This is also the case for the total field strength.

For a standing wave, the Poynting flux of the incident wave is balanced with that of the reflected wave. In other words, the field-aligned component of the Poynting flux should be averaged out over a wave period, which requires a 90° phase lag between electric field and magnetic field variations. Here the combination to be examined for the present event is B_Y and E_X; note that the background magnetic field was directed approximately in the z direction. However, no systematic phase lag between B_Y and E_X can be found in Figure 3.

Figure 5 shows the result of the coherence analysis between B_Y and E_X [*Bendat and Piersol*, 1971]; the interval of 1345 to 1515 UT was selected for the analysis. The PSDs of (a) B_Y and (b) E_X, and (c) coherence and (d) cross phase between the two are plotted. Although the PSD of E_X suggests an enhancement around 3.3 mHz, the coherence between B_Y and E_X is less than 0.4 around this frequency, and eventually we could not determine the cross phase reliably. This result suggests that the energy associated with this 5-min oscillation was not confined in a magnetic flux tube. In other words, the oscillation was continuously excited, and Geotail was likely in or very close to the excitation region.

Figure 6 compares the x and y components of the electric drift velocity for the same interval as in Figure 4. The phase of V_Y was roughly 90° ahead of that of V_X except during 1415 to 1430 UT. That is, the flow velocity rotated clockwise with time in the x–y plane in the view from the north. The polarization is consistent with the idea that the oscillation was excited by a boundary process at

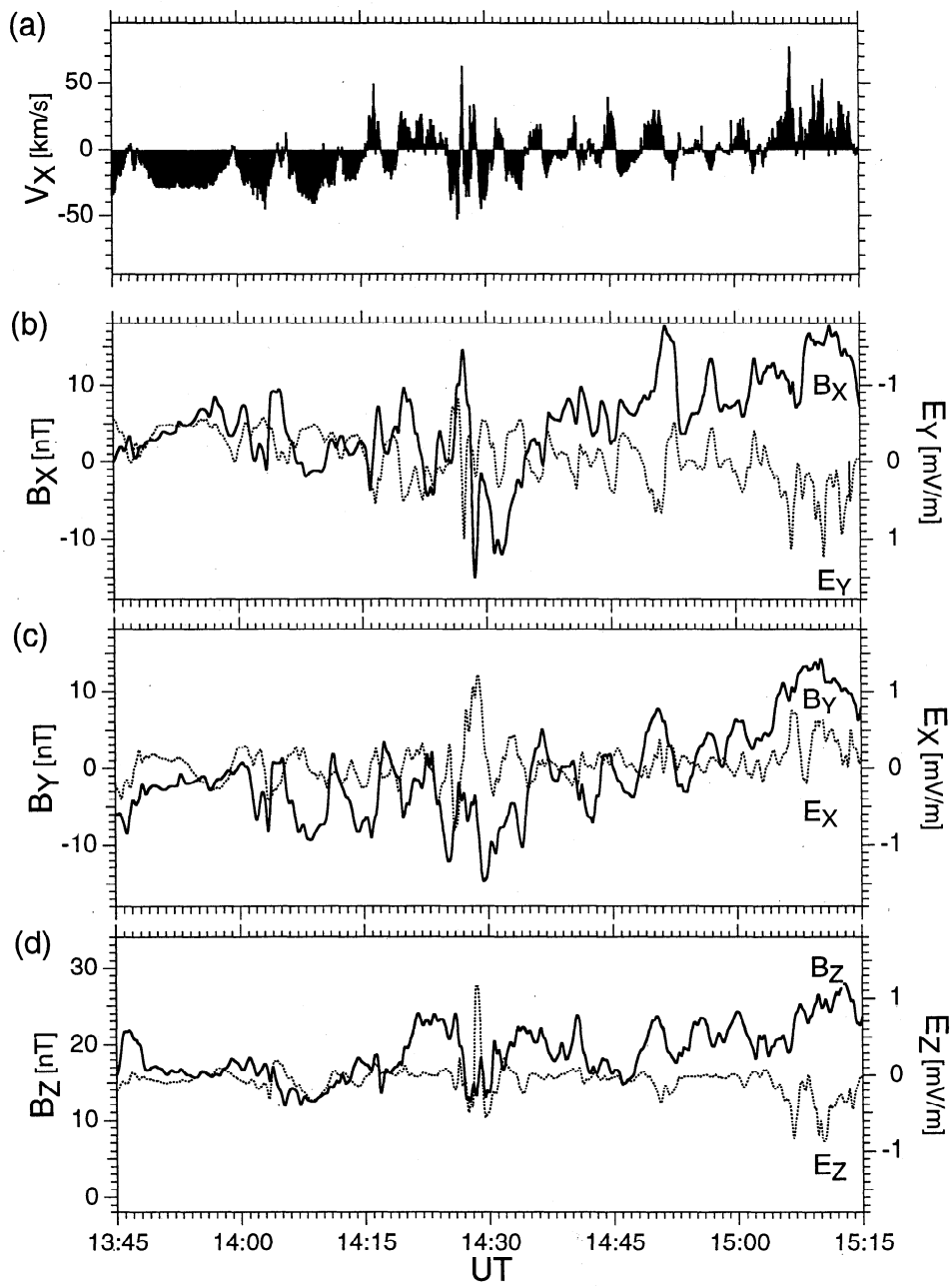

Figure 3. Geotail electric field and magnetic field data. (a) The x component of the electric field drift. (b) B_X (solid line) and E_Y (dotted line). (c) B_Y (solid line) and E_X (dotted ine). (d) B_Z (solid line) and E_Z (dotted line).

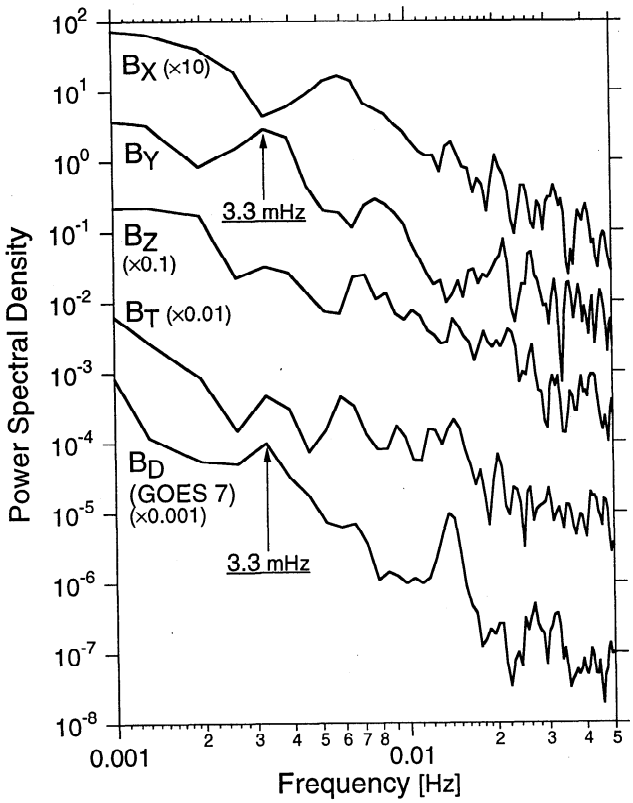

Figure 4. The power spectral density of the three magnetic field components and the total field strength observed by Geotail for 1405 to 1456 UT. Also plotted is the power spectral density of the GOES 7 *D* magnetic component. The plots are slid vertically for comparison by a factor indicated in parentheses.

the morningside flank of the magnetosphere. However, we cannot tell from the single-point measurement whether or not the wave had a spatial vortex structure; for a surface wave, the flow vector rotates at a fixed point, but the vector field does not necessarily have finite vorticity [*Atkinson and Watanabe*, 1966]. From a peak-to-peak amplitude of the velocity oscillation, $\delta v = 30$ km/s, and a wave period of T = 5 min, the displacement of a fluid element is estimated to be 1400 km ($= \delta v \cdot T/2\pi$) at the Geotail position.

2.3. Geosynchronous Signatures

Figure 7 plots the GOES 7 magnetometer data in *V*, *D*, and *H* (Figure 7a, b, and c, respectively) coordinates (see Figure 1; the satellite was located at a magnetic latitude of 7.6°). In this coordinate system, *H* is antiparallel to the dipole axis, *V* points radially outward and is parallel to the magnetic equator, and *D* completes a right-hand orthogonal system (positive eastward). Note that the scale of the *V* and the *D* components is half that of the *H* component.

Quasi-periodic fluctuations of 5 min were evident in the azimuthal (*D*) component until 1440 UT (Figure 7b). Similar fluctuations can barely be seen in the *V* component (Figure 7a) but cannot be seen at all in the *H* component (Figure 7c). That is, the oscillation was transverse to the magnetic field and was polarized linearly in the azimuthal direction. The dashed line in Figure 7b represents the Geotail B_Y component. The scale for the Geotail data, which is four times that of the GOES 7 *D* component, is given on the right-hand side. The time of the Geotail data is shifted backward by 120 s. The agreement of the timings of peaks is surprisingly good between the two plots, and the PSD of the GOES 7 *D* component (Figure 4) has a peak at 3.3 mHz. For the later interval, the 5-min oscillation was less clear at GOES 7 partly because of the superposition of higher-frequency variations.

There are two important differences between the GOES 7 and Geotail signatures. First, the amplitude of the fluctuations was much smaller at GOES 7. The peak-to-peak amplitude was a few nT at GOES 7, whereas it was about 10 nT at Geotail. Second, the direction of the wave polarization was different at the two satellite positions. At GOES 7 the oscillation was polarized in the azimuthal direction, which is close to the GSM *x*, rather than *y*, direction at the local time of GOES 7 (Figure 1a), whereas at Geotail the magnetic oscillation was polarized in the GSM *y* direction. If the oscillation is described, at least locally, as a shear Alfvén wave,

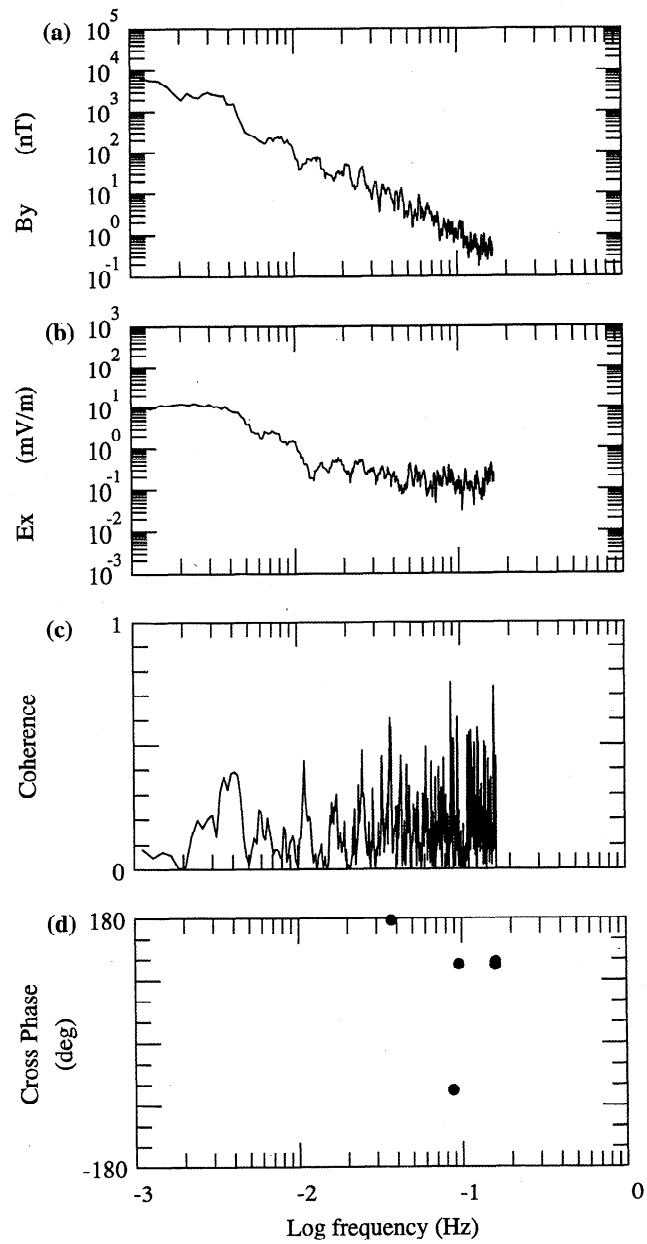

Figure 5. Comparison of the Geotail B_Y and E_X data for the interval of 1345 to 1515. Plotted are (a) the power spectral density of B_Y, (b) that of E_X, (c) the coherence, and (d) the cross phase between the two. The N band was chosen to be 9.

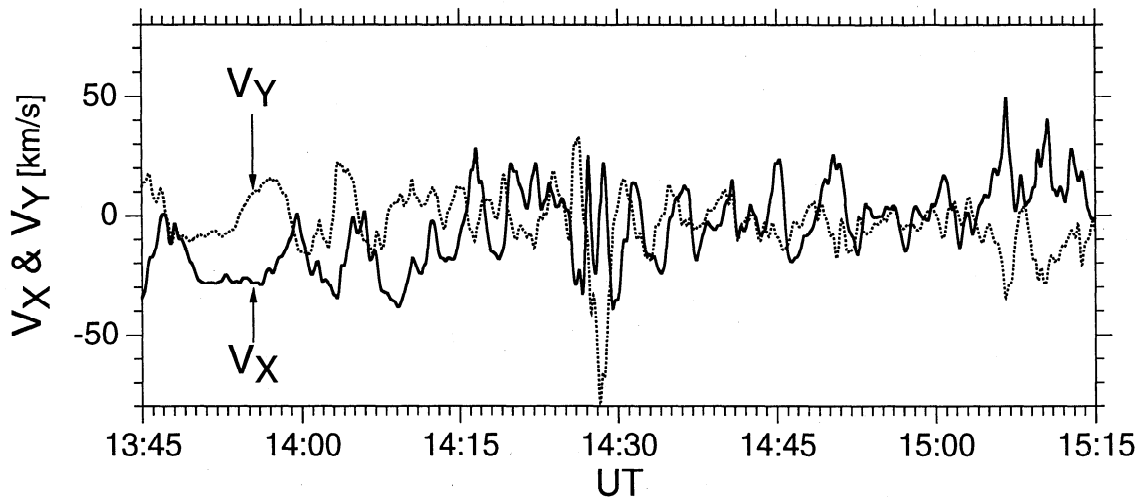

Figure 6. The GSM x (solid line) and y (dashed line) components of the electric field drift calculated from the Geotail electric field and magnetic field measurements.

this fact indicates that the variation of the wave phase was in the x direction in the boundary region, whereas it was in the radial (y) direction in the geosynchronous region.

Figure 8 shows the Fast Fourier Transform (FFT) dynamic spectrum of the GOES 7 D component for the 1-hour interval of 1400 to 1500 UT. The window used for the FFT is 128 data points (384 s). A harmonic structure is most evident for the interval of 1430 to 1440 UT, which is similar to those reported by *Takahashi and McPherron* [1982]. Four discrete bands can be recognized. They are around 15, 32, 50, and 65 mHz. Because GOES 7 was off the equator (7.6° in magnetic latitude; the magnitude of the V component was several tens of nT as shown in Figure 7a), it is unlikely that the satellite observed only even modes. Therefore, we infer that 15 mHz is the eigenfrequency of the fundamental mode, and the others are its higher (second, third, and fourth) harmonics. Each band shifts to a lower frequency as we go back in time, and it is more difficult to determine the fundamental frequency for an earlier period. However, we note that the harmonics are separated by at least 10 mHz. Since the frequency separation (Δf) between harmonics is expected to be close to the eigenfrequency of the fundamental mode (f_1) [*Cummings et al.*, 1969], we can dismiss the possibility that the observed 5-min (3.3 mHz) oscillation was coupled to a standing mode of the GOES 7 field line. If such a coupling took place in the present event, we expect that the resonance shell was located outside of geosynchronous orbit.

We also examined GOES 6 magnetic field measurements (not shown) and found that one spin-plane component oscillated at the same frequency. The oscillation was transverse to the ambient magnetic field. For several corresponding signatures observed by both GOES satellites, the phase was ahead at GOES 6 by an amount corresponding to a time delay of 30 to 90 s, indicating the antisunward propagation of the wave.

Figure 9 plots the total magnetic field strength measured at Geotail, GOES 6 and GOES 7, and the H (horizontal) magnetic component at the Hermanus ground station, which was located in the afternoon sector (PACE Geomagnetic Latitude: –42.2°; Geomagnetic Longitude: 82.1°; MLT = 14.9 at 1430 UT). For Geotail B_T the initially smoothed data (45-s binomial sliding averages based on 3-s data) are plotted by the dashed line, whereas the further smoothed data (5-min running averages) are plotted by the solid line. The sampling rate of the Hermanus data is 1 min, and the 3-s three-component measurements were used for calculating B_T for the GOES satellites. The scale is the same for all plots, but the baseline is offset as denoted in the figure.

The similarity between the two GOES plots is remarkable. The Hermanus H component also changed in a very similar way. Therefore, those variations were global and most likely reflected changes in the external pressure. We emphasize that none of those plots indicate a 5-min oscillation. The plot of Geotail B_T (the dashed line) is more structured, presumably because Geotail observed spatial, as well as temporal, effects associated with the satellite motion relative to the magnetopause. However, more importantly, the overall feature of the long timescale variations (the solid line) at Geotail was similar to the signature observed at GOES and Hermanus, indicating that the local condition at Geotail was also affected by changes in the external pressure. The transient decrease in B_T (B_Z; see Figure 3d) around 1430 UT that we mentioned previously is one of such changes. However, we infer that the 5-min oscillation we observed was not an effect, at least not a direct effect, of the variation of the external pressure.

2.4. Ground Signatures

Figures 10 and 11 plot the differentiated x (northward) and y (eastward) magnetic components, respectively, from ground stations along the higher-latitude east-west chain from PG to CON (Figures 10a and 11a), the meridional chain from RAN to PIN (Figures 10b and 11b), and the lower-latitude east-west chain from GIL to SIM (Figures 10c and 11c; see Figure 1b). The time resolution of the data is 5 s. Figure 12 shows the PSDs of measurements from the stations of the lower- and higher-latitude east-west chain for the interval of 1405 to 1450 UT; the sum of the PSDs of the differentiated x and y magnetic components is plotted. Figure 12 also shows the PSDs of the Geotail and GOES 7 measurements. The plots are shifted arbitrarily in the vertical direction, whereas the logarithmic value of the PSD at 3.1 mHz is given for each station in the figure. This is the dominant frequency of ground signatures and agrees with the frequency of the Geotail B_Y and GOES 7 D oscillations, 3.3 mHz, within the resolution of the FFT analysis, $\Delta f = 0.78$ mHz.

Among the four stations shown in Figures 10a and 11a, RAN observed 5-min oscillations most clearly. At the eastward-most station, PG, which was in the prenoon sector, the characteristic timescale of fluctuations was much shorter. At CD, which was located between

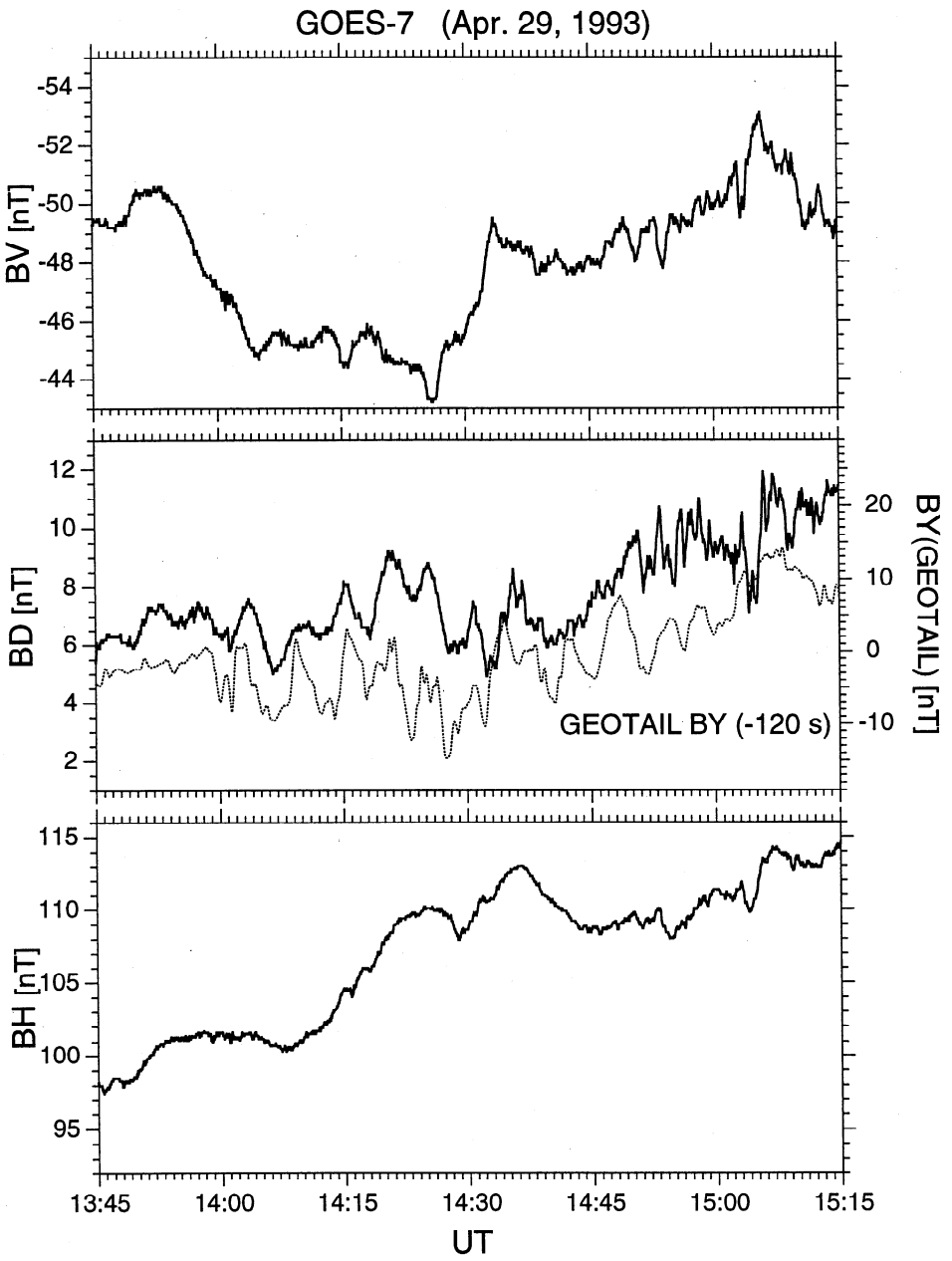

Figure 7. The GOES 7 (a) V, (b) D, and (c) H magnetic components. The scale for the V and D components is half that of the H component. The dashed line in panel (b) is the Geotail B_Y component, shifted 120 s backward. The scale for the Geotail data is given on the right-hand side of the panel.

PG and RAN in longitude, the signature was intermediate; high-frequency oscillations were superposed on more slowly varying oscillations. At CON, westward of RAN, magnetic pulsations were less clear, although some undulations were observed.

These features can also be seen in Figure 12 (the top four plots). The *Pc5* wave observed at RAN corresponds to the spectral peak at 3.1 mHz. The PSD of CD has a kink, rather than a peak, at 3.1 mHz, whereas we cannot find any clear indication in the PSD of PG. The tendency of the PSD at 3.1 mHz to increase from PG to RAN may be interpreted in terms of the growth of a wave as it propagates from the dayside; the antisunward propagation of the wave will be confirmed later. We speculate that CON was located in the open field line region.

Pc5 pulsations were clearly observed along the meridional chain (Figures 10b and 11b), although the amplitude was significantly smaller at ISL and PIN, especially in the y component. The most prominent feature was the continuous oscillation during the interval of 1415 to 1440 UT. The oscillation period was approximately 5 min. After the intermittence of one or two wave periods, the oscillation appeared again, though with smaller amplitudes.

Figure 13 shows the amplitudes (top) and phases (bottom) of the 3.1 mHz Fourier components of the differentiated x (solid lines) and y (dashed lines) magnetic components observed along the meridional chain during 1415 to 1440 UT. The amplitude of the y-component variations increased monotonically with latitude, and the phase was more or less constant. In contrast, the amplitude of the x component had a local maximum around BAC and GIL, and its phase changed by 180° throughout the meridional chain (see the dashed lines in Figure 10b). Although one may attempt to explain these features in terms of the field line resonance theory [*Southwood*, 1974; *Chen and*

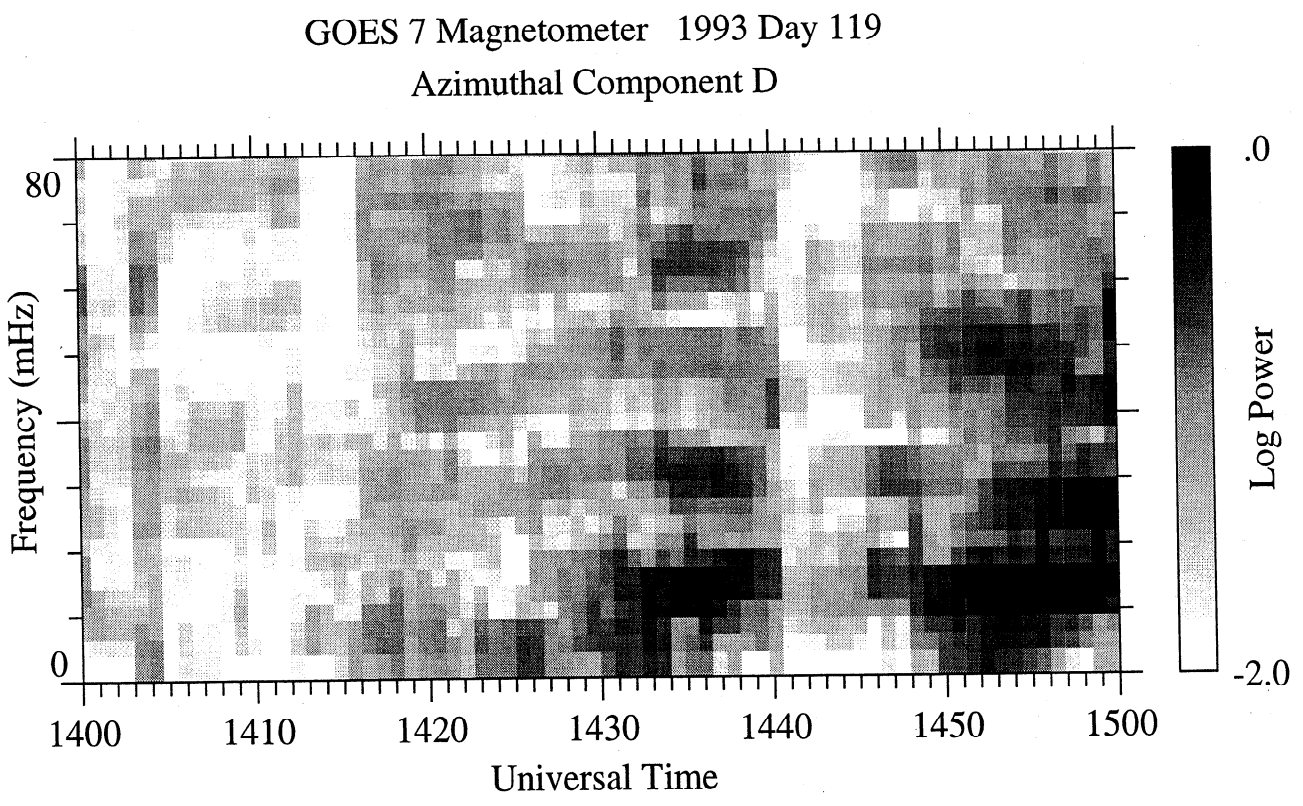

Figure 8. The FFT dynamic spectrum of the GOES 7 *D* component for the 1-hour interval of 1400–1500 UT.

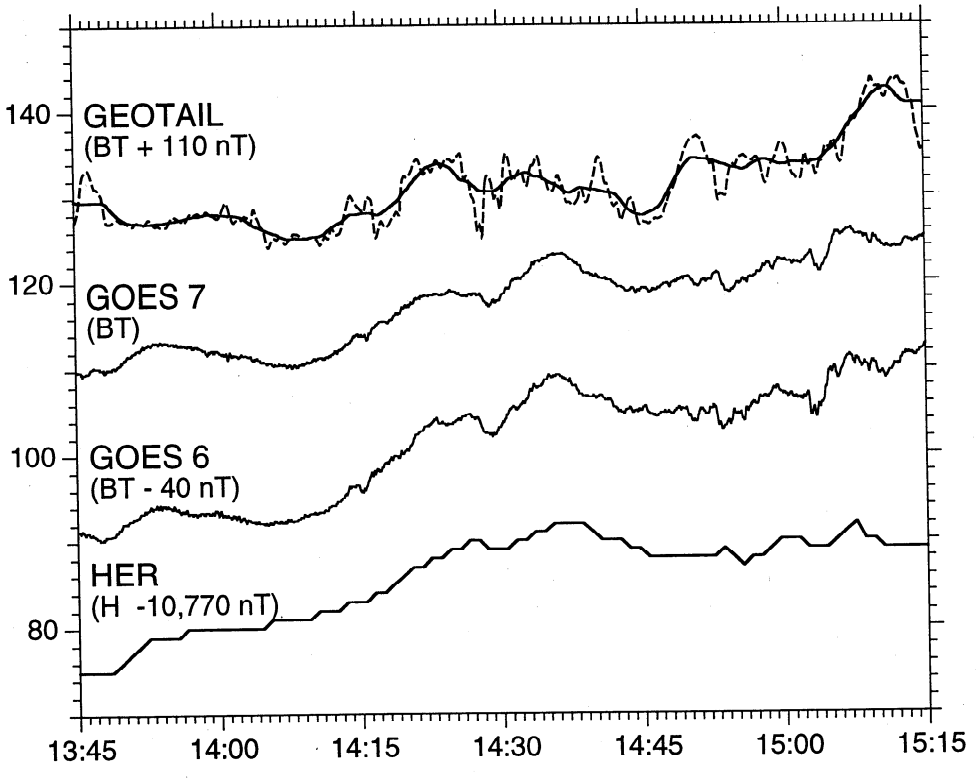

Figure 9. The total magnetic field strength measured at Geotail, GOES 6, GOES 7, and the *H* (horizontal) magnetic component at Hermanus during 1345–1515 UT of April 29, 1993.

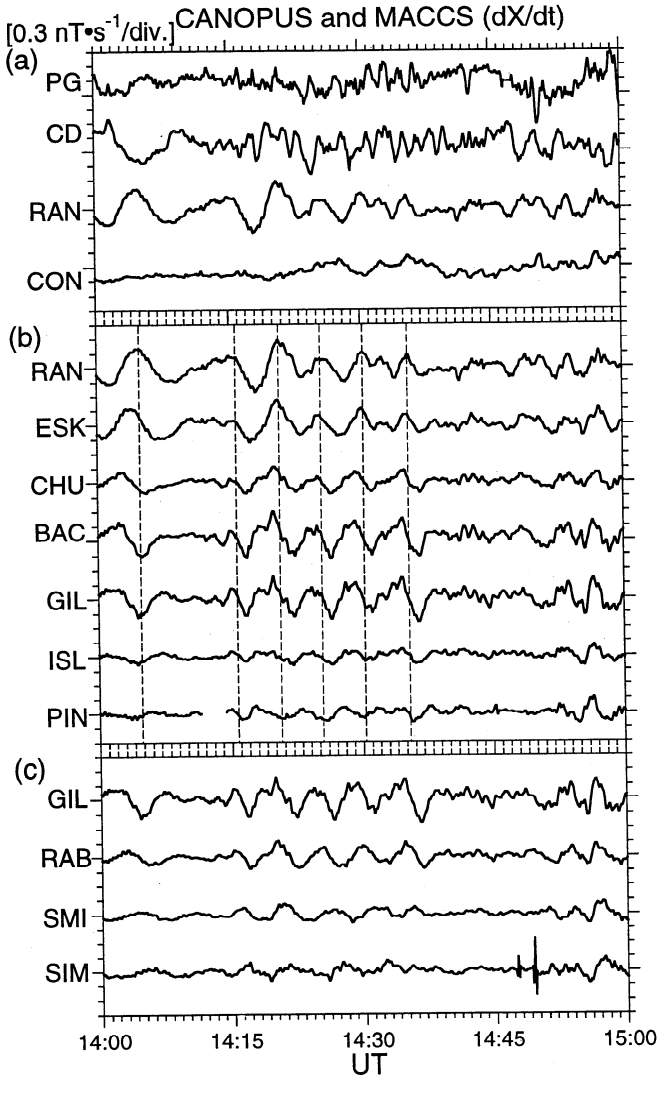

Figure 10. The differentiated x-component magnetic field data measured at ground stations along (a) the higher-latitude east-west chain of PG to CON, (b) the meridional chain from RAN to PIN, and (c) the lower-latitude east-west chain from GIL to SIM (see Figure 1b and Table 1).

Hasegawa, 1974], there are a few difficulties with this approach. First, the 180° phase change was not localized around the local maximum of the amplitude but occurred gradually. This is a remarkable contrast to previously reported events [*Samson et al.*, 1971; *Greenwald and Walker*, 1980; *Singer et al.*, 1982]. More importantly, the phase tended to be ahead at lower latitudes, which is just opposite to what the field line resonance theory predicts for a resonance point. Instead, despite the local maximum of the amplitude, the sense of the phase shift was the same as the theory predicts for the local minimum of the amplitude [see *Southwood*, 1974, Figure 2]. We could not think of any plausible reason for this puzzling feature.

The latitudinal variation of a wave polarization along the meridional chain is examined in Figure 14, which shows the hodograms of linearly detrended magnetic variations in the x-y plane observed at RAN, CHU, BAC, GIL, ISL, and PIN during 1427:00 to 1431:30 UT. Here we used the original, not differentiated, data. Note that in each panel, the vertical (horizontal) axis represents the x (y) component so that the top (right) of the panel is northward (eastward). The scale for the ISL and PIN measurements is less than half that for the other stations.

The polarization of the wave was almost linear at RAN. The result of the cross-phase analysis [*Waters et al.*, 1995] between RAN and ESK indicates that one of the resonance frequencies at that latitude was about 3.3 mHz (not shown). Therefore, it is likely that the field line resonance took place near the L shell of RAN; this is consistent with the result of the analysis of the GOES 7 data (section 2.2) that the resonance shell, if it existed, was located outside of geosynchronous orbit and therefore, on the ground, poleward of GIL. At CHU the hodogram was more circular and the polarization was counterclockwise. The polarization was also counterclockwise at the lower-latitude stations except the equatorward-most station (PIN), where the oscillation was polarized linearly in the x direction. The counterclockwise rotation on the ground is projected to the equatorial plane as the clockwise rotation in the view from the north, which is the same polarization of the flow velocity rotation observed at Geotail.

The 5-min oscillation was also clearly observed along the lower-latitude east-west chain (Figures 10c and 11c). RAB, SMI, and SIM were close to the footpoint of Geotail (Figure 1b). Again, the peak frequency of the PSDs of these stations was 3.1 mHz.

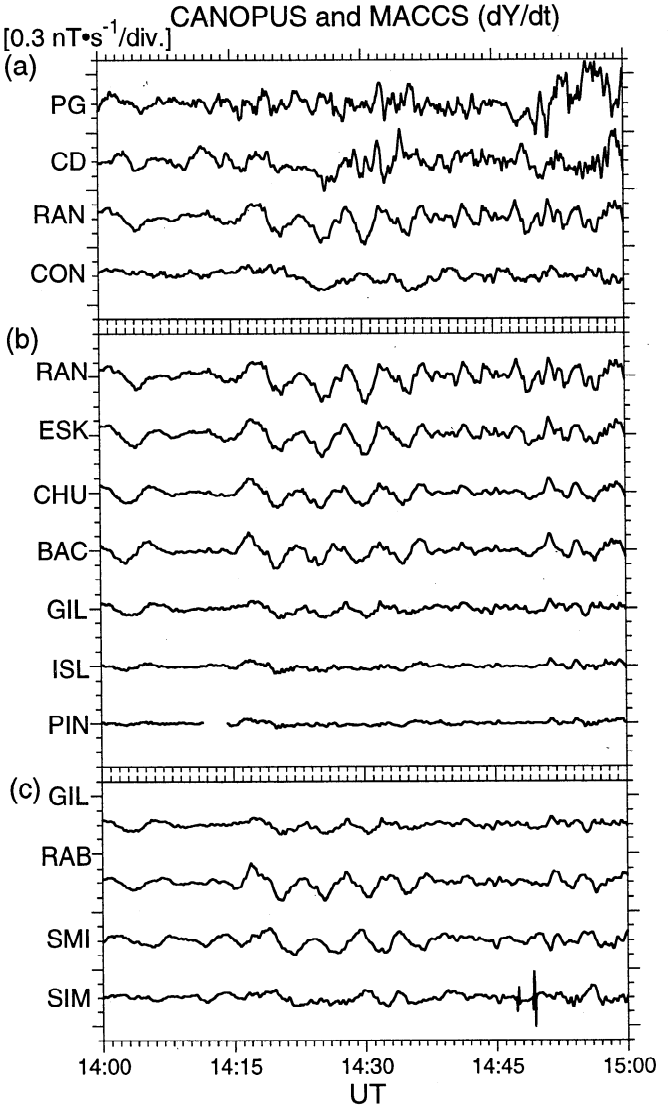

Figure 11. The differentiated y-component ground magnetometer data. The format is the same as in Figure 10.

RAB was closest to the footpoint of GOES 7. The PSDs for these two locations are compared at the bottom of Figure 12. In addition to the peak at 3.1 mHz, we can see a possibly corresponding peak at 14 mHz, as marked by the solid triangle in Figure 12, which we inferred previously (section 2.2) to be the fundamental eigen-frequency of the GOES 7 field line.

We examined the correlation between measurements (dB_X/dt and dB_Y/dt) at each station of this east-west chain and the corresponding component at RAN for the interval of 1410 to 1440 UT. Figure 15 plots the obtained time lags (Δt) against the magnetic longitudes using solid circles for dB_X/dt and solid squares for dB_Y/dt. The correlation was found to be higher than 0.5, except for dB_X/dt of SIM, which is excluded from Figure 15. We did the same analysis for BAC, and the results are shown by the open circle (dB_X/dt) and open square (dB_Y/dt).

The decrease toward the right indicates that the signals propagated westward (antisunward). The tendency is opposite for dB_Y/dt between RAB and GIL. This is ascribed to the possible mixture of latitudinal and longitudinal structures. Note that the time lag was different by more than 40 s between BAC and GIL, which are separated by only 1.4° in latitude (see also Figure 13). From the least squares fit, the slopes of the plots are estimated at 3.1 and 3.0 (3.9) s/deg for dB_X/dt and dB_Y/dt (dB_Y/dt, but with BAC instead of GIL), respectively. By taking the average of these three estimates, the propagation velocity is estimated at 18°/min, which corresponds to 400 km/s at a radial distance of 13 R_E (the magnetopause distance

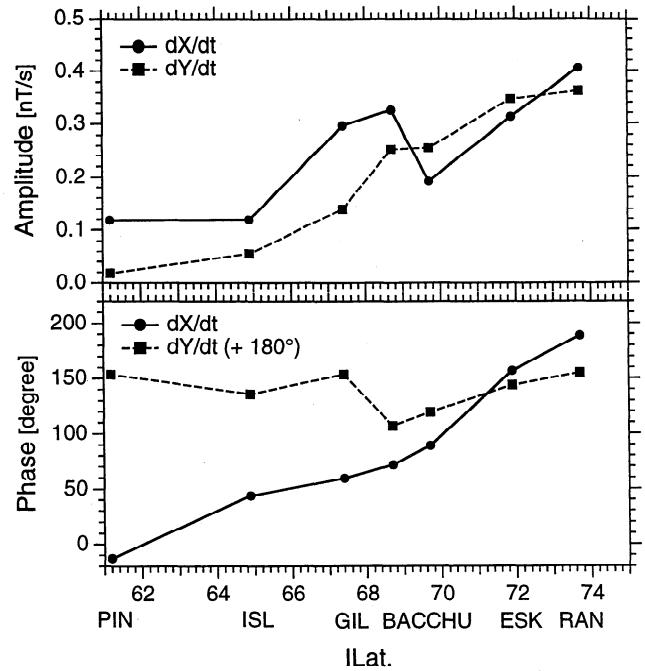

Figure 13. The (top) amplitudes and (bottom) phases of the differentiated x (solid lines) and y (dashed lines) magnetic components observed along the meridional chain.

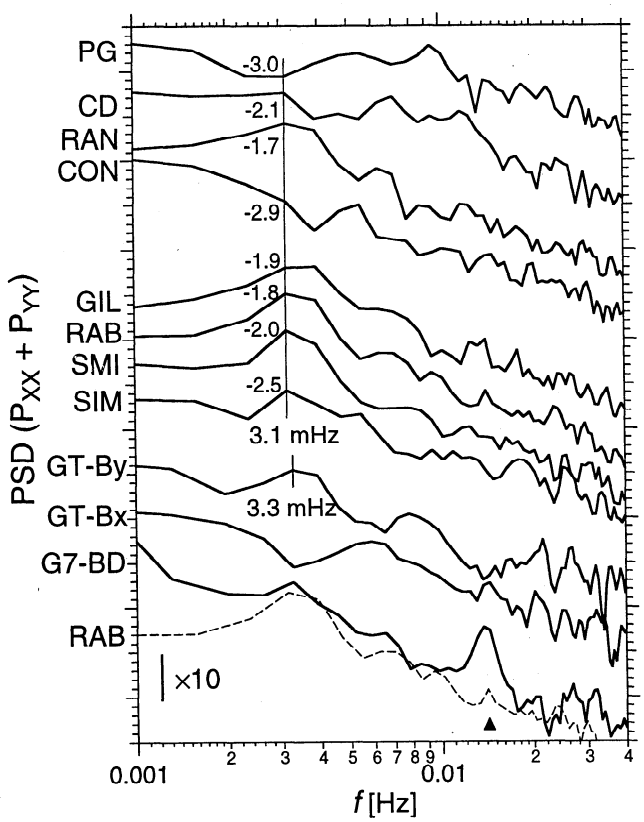

Figure 12. The PSDs of the ground magnetometer data along the higher- and lower-latitude east-west chains. The sum of the PSDs of the x and y components is plotted. The logarithmic value of the PSD at 3.1 mHz is given for each station. The PSDs of the Geotail and GOES 7 measurements are also plotted in the bottom part of the figure.

at the local time of GOES 7; see Figure 1). By multiplying a wave period of 5 min, the longitudinal characteristic length is estimated to be 90°, or 1.2×10^5 km (19 R_E). Although these estimates depend on the mapping and therefore should be treated with caution, we will later find that our estimates are consistent with the previous results. We also note that the propagation velocity is 200 km/s, if mapped to geosynchronous altitude (the GOES 7 footpoint was close to the east-west chain in latitude), which is significantly smaller than the typical propagation speed (> 1000 km/s) of the fast magnetosonic wave. Therefore, the observed pulsation cannot be explained in terms of an effect of external compression propagating from the dayside.

2.5. Freja Observations

The Freja satellite [*Lundin et al.*, 1994] passed over the same region of the ground stations during the interval of 1430 to 1450 UT (Figure 1a). Figure 16 plots the north-south (B_N; positive northward) and east-west (B_E; positive eastward) components of the Freja magnetometer data [*Zanetti et al.*, 1994]. The B_E component tended to decrease from 1436 to 1442 UT and then increase until 1445 UT. Both slopes indicate the satellite skimming of a single upward flowing field-aligned current (FAC) sheet; the satellite reached the highest invariant latitude at 1442 UT (Figure 1a), when B_E became minimum. This FAC is inferred from its polarity (upward) to be a morningside region 2 current. The Freja particle instrument [*Eliasson et al.*, 1994] observed the precipitation of ions in the energy range of 0.1–100 keV during the same interval (not shown), which was presumably the CPS [*Winningham et al.*, 1975]. The corresponding orbital segment is represented by the thick line in Figure 1b. Note that the 5-min oscillation was observed at ISL and even at PIN further equatorward of the region 2 FAC and CPS. Similar events were observed previously by the Viking satellite [*Potemra and Blomberg*, 1996].

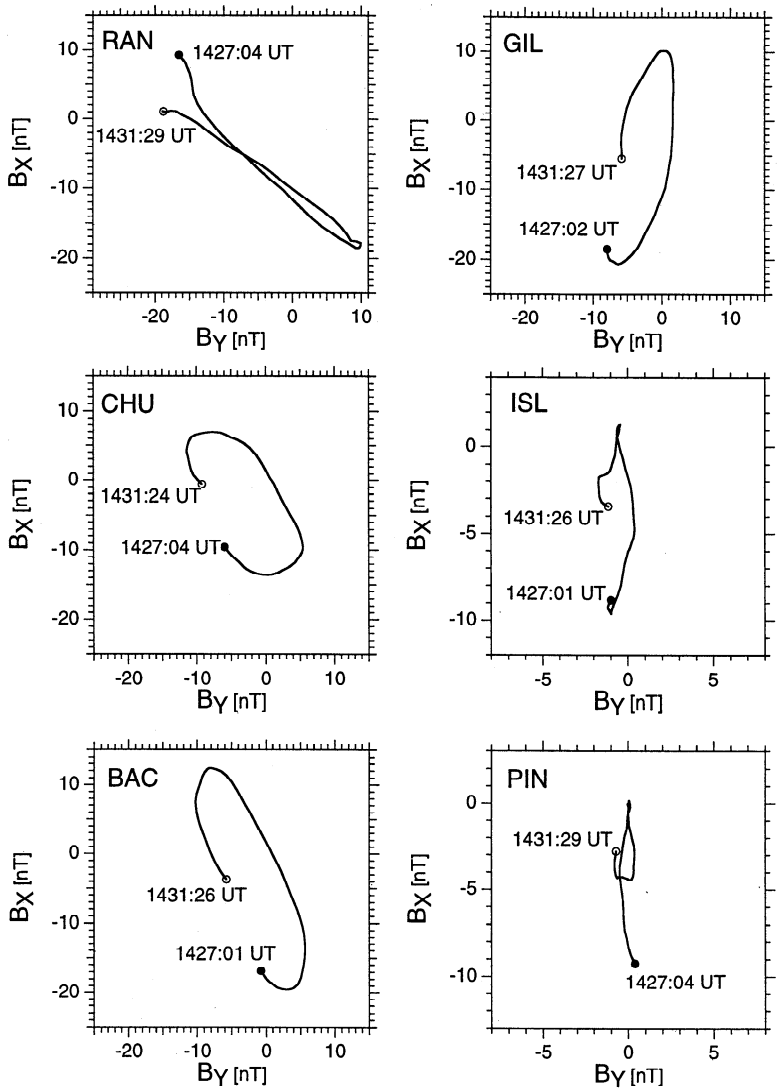

Figure 14. The hodograms of magnetic perturbations in the x–y plane observed at RAN, CHU, BAC, GIL, ISL, and PIN.

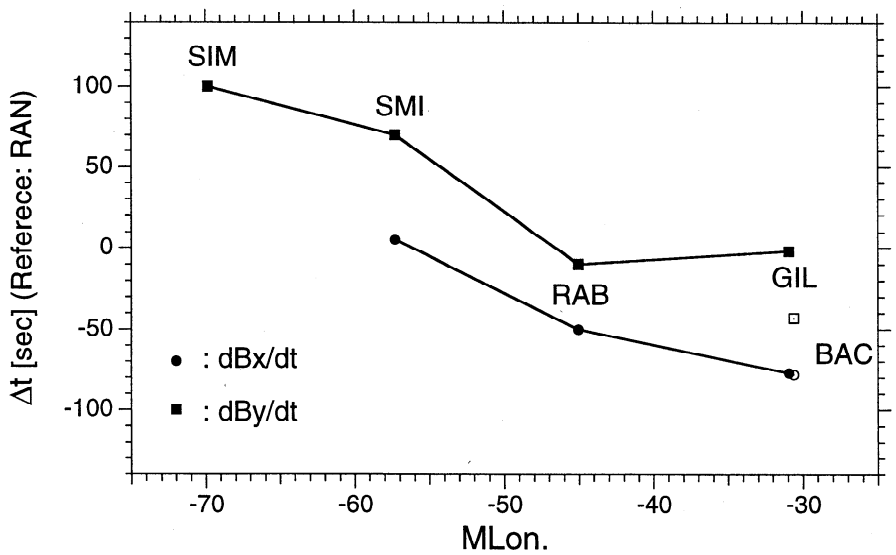

Figure 15. The phase lag of the differentiated x (solid circles) and y (solid squares) components measured at the four ground stations along the lower-latitude east-west chain for the interval of 1410 to 1440 UT. The corresponding component of RAN is used as a reference for the correlation analysis. The open circle and square not connected by a segment represent the result for the differentiated x and y components, respectively, of BAC.

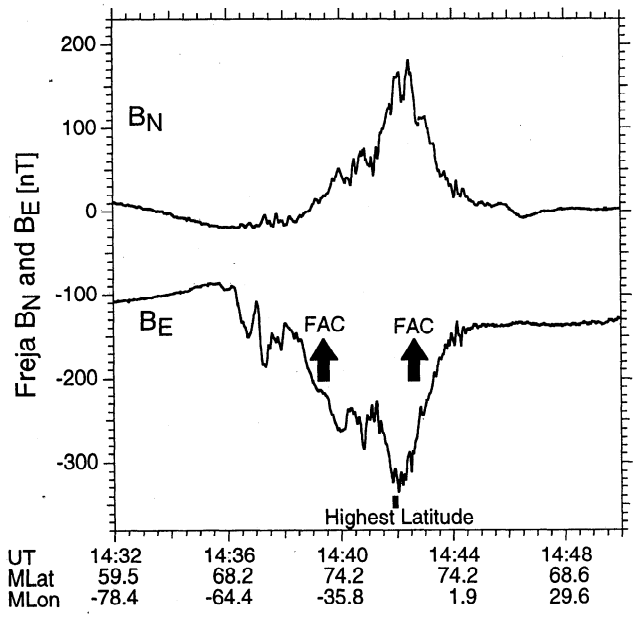

Figure 16. The Freja north-south and east-west magnetic components. See Figure 1b for the orbit trajectory.

3. Discussion

3.1. Comparison with Previous Studies

In the present event, Geotail observed 5-min magnetic oscillations at the flank of the magnetosphere. This magnetic pulsation is accompanied by the clockwise rotation of the plasma flow vector (Figure 6). A similar feature was reported for a class of magnetospheric low-frequency pulsations called plasma vortex event [e.g., *Hones et al.*, 1978]. However, the present event should be distinguished from a plasma vortex event. In a plasma vortex event, the plasma flow rotates in a plane including the background magnetic field and is therefore partly parallel to the magnetic field. In contrast, the flow velocity we examined with the Geotail data is perpendicular to the ambient magnetic field, which may be more intuitively understood in terms of a surface wave.

The absence of a clear 90° phase lag between the Geotail magnetic field and electric field variations indicates that the observed oscillation is not a standing wave (Figure 5). In contrast, *Nakamura et al.* [1994] found a 90° phase lag between magnetic field and electric field oscillations for a *Pc*5 event also observed by Geotail near the dayside magnetopause. They inferred that the wave was excited by a sudden change in the solar wind (magnetosheath) pressure. A pulsation excited impulsively may establish a standing structure more easily than one excited continuously, because the characteristics of the latter, such as a wave period, are determined by those of the wave source. We infer that the present event is an example of the latter case.

A few studies have examined boundary waves with multisatellite observations in different areas of the magnetosphere [*Takahashi et al.*, 1991; *Chen et al.*, 1993; *Sarafopoulos*, 1993]. *Takahashi et al.* [1991] reported an event in which transverse oscillations were observed only near the magnetopause, whereas compressional oscillations were observed much more globally. They inferred that the former is excited by the K-H instability, whereas the latter is associated with external pressure variations. In contrast, in the April 29, 1993, event, the correspondence between the Geotail and GOES signatures was better during the first interval, when the oscillation at Geotail was transverse, than during the second interval, when it was partly compressional. We infer that the excitation mechanism operates more globally for the first interval; we will discuss the excitation mechanism in section 3.2.

One might think that the 5-min oscillation during the second interval, which was compressional as well as transverse at Geotail, was caused by variations in the external pressure. The previous studies [*Sibeck et al.*, 1989; *Fairfield et al.*, 1990] have shown that in the dayside magnetosphere, the total field strength can change periodically in response to variations in the external pressure that are not inherent in the solar wind but are produced by an interaction between the bow shock and the magnetopause. In the present event, however, the GOES satellites (Figure 8) did not observe any clear variation of B_T that can be associated with the 5-min B_T oscillation at Geotail, even though they were located closer to the subsolar point than Geotail. Therefore, we conclude that the present event is different from the pressure-driven phenomenon reported previously.

Table 2 lists several physical quantities reported previously for boundary waves observed at or near the magnetopause in the morning sector, including the present event. The studies are listed in the decreasing order of the x coordinate of a satellite observation point. Whereas the present study estimates the propagation speed and longitudinal characteristic length (wavelength) from the ground observations, other studies determined these quantities from a model fitting [*Lepping and Burlaga*, 1979] or from a timing study of dual

Table 2. Summary of Previous Studies on Morningside Low-Frequency Pulsations Observed Close to the Magnetopause

Reference	X, R_E	Period, min	Velocity, km/s	Wavelength, R_E	Amplitude, R_E
Sckopke et al. [1981]	+5	2–5	—	3–8	1
Takahashi et al. [1991]	+ 2–3	0.8	—	—	—
Kokubun et al. [1994b]	–1.5	2.6	—	3	—
Lepping and Burlaga [1979]	–3	2.8	340	7–8	0.3
This paper	–6	5	400[1]	19[1]	0.2[2]
Chen and Kivelson [1993]	–8	3-8	—	3-8	0.3–0.7
Couzens et al. [1985][3]	–15	3-4	350	6–7	0.8
Chen et al. [1993]	–15	5	300–350	15	—
Geotail Day 024, 1994	–31	10	—	—	—

[1]Estimated from the ground observations.
[2]Amplitude in the LLBL.
[3]An event observed at the dawnside flank.

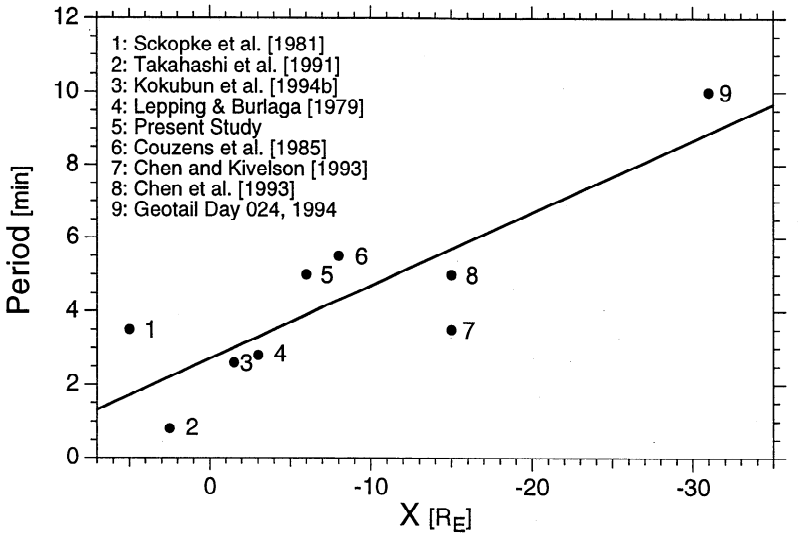

Figure 17. The periods of boundary waves reported in the previous studies plotted against the x coordinates of observation points.

satellite observations [*Couzens et al.*, 1985; *Chen et al.*, 1993]. The wave amplitude of the present event is likely to be underestimated since Geotail stayed inside the magnetosphere; the amplitude of a boundary wave should be evanescent inward from the magnetopause. The event listed at the bottom of the table has not been reported before. For the interval of 1430 to 1630 UT on day 024 of 1994, Geotail was in the vicinity of the magnetosheath-magnetosphere boundary on the dawn side. The satellite observed a quasi-periodic oscillation in the magnetic field and plasma bulk parameters, which we attribute to a coherent radial motion of the boundary.

There are three points to be noted in Table 2. First, the propagation speed is comparable to the expected flow speed of the magnetosheath. Second, the longitudinal characteristic length (wavelength) is of the same order as the x distance of the spacecraft from the subsolar point. The last point, which is less clear than the preceding ones, is that the oscillation period tends to be longer as the observation is made farther away from the subsolar point. Figure 17 plots the oscillation period as a function of the x coordinate of the spacecraft location. The solid line represents the result of the line fitting; $T = -0.20\ (\pm 0.04) \times x + 2.7\ (\pm 0.6)$, where x and T are in units of R_E and minutes, respectively. The result shows a positive trend. Although a significant contribution to the line fit is made by the data point labeled 9 because of its largest distance, the tendency to increase can also be seen for the remaining eight data points. Thus, there is no clear discrepancy between the determined parameters of the present event and those of boundary waves reported previously, strongly suggesting that the 5-min oscillation we examined was also a boundary wave.

3.2. Excitation Mechanism

The external excitation of *Pc5* waves has been discussed in terms of two models, that is, the K-H instability (references cited in section 1) and the external pressure variation [e.g., Sibeck *et al.*, 1989; *Fairfield et al.*, 1990]; in addition, there may be a class of *Pc5* waves associated with the field line merging [*Song et al.*, 1988]. These mechanisms are not necessarily exclusive, but perhaps can operate simultaneously at different frequencies [*Takahashi et al.*, 1991; *Ziesolleck and McDiarmid*, 1994]. This might also be the case for the present event. However, concerning the 5-min oscillation on which we have been focusing, we infer that the K-H instability is more probable than the external pressure variation as the excitation mechanism. There are four reasons for this: (1) the rotation of the plasma flow velocity observed by Geotail, (2) no clear compressional signature at Geotail (except during 1445 to 1500 UT), (3) the absence of corresponding compressional magnetic variations at the GOES satellites, and (4) the antisunward propagation of the wave at a velocity similar to the magnetosheath flow velocity. In addition, we discussed in the previous section that the 5-min oscillation during the second interval is different from events previously reported to be driven by external pressure variations.

Sckopke et al. [1981] reported an event for which they suggested that the inner edge of the boundary layer rather than the magnetopause is unstable to the K-H instability (see *Kivelson and Chen* [1995] for an alternative interpretation of the event). A similar model was also discussed to explain periodic auroral structures observed at the flank of the oval [*Rostoker et al.*, 1992]. *Ogilvie and Fitzenreiter* [1989] tested the incompressible hydromagnetic stability condition for the K-H instability [*Hasegawa*, 1975] and found that a transition layer inside, or at the inner edge of, the LLBL is more likely to be unstable against the instability, while the magnetopause is more stable. However, as pointed out by *Miura* [1992], some caution is necessary for their result since the plasma and magnetic field parameters they tested may represent those at a nonlinear saturation stage of the K-H instability.

There is a significant difficulty in explaining the Geotail observation of the present event in terms of the K-H instability at the inner edge of the LLBL. The phase velocity of a K-H mode V_{ph} is given as the average of flow velocities V_i (i = 1, 2, indicating a different side of the boundary) weighted with a mass density ρ_i on each side of the velocity shear,

$$V_{ph} = \frac{\rho_1 V_1 + \rho_2 V_2}{\rho_1 + \rho_2}. \quad (1)$$

Thus, if a K-H mode is excited at the inner boundary of the LLBL, its phase velocity should not exceed the flow velocity of the LLBL, which is even lower than the flow velocity of the magnetosheath. However, for the present event the propagation velocity of the wave is inferred to be comparable to the flow speed of the magnetosheath (section 2.3). Actually, this discrepancy can also be found for events reported previously (Table 2). (If plasma was convected at

400 km/s in the LLBL, the cross potential difference across the LLBL would be 50 keV, or 100 keV if combined with the duskside LLBL, for a magnetic field strength of 20 nT and a thickness of the LLBL of 1 R_E. This is improbable.)

Whereas *Ogilvie and Fitzenreiter* [1989] tested the instability criterion for a boundary between two plasma regions, *Lee et al.* [1981] investigated the K-H stability of a three-layer structure: the magnetosheath, the boundary layer, and the magnetosphere. They found that there are two unstable modes. One is excited at the magnetopause (the magnetopause mode) and the other at the inner edge of the boundary layer (the inner mode). Whereas the inner mode can be unstable more often, the stability of the magnetopause mode is more sensitive to magnetosheath parameters, especially the orientation of the magnetic field.

When the magnetosheath magnetic field is directed northward, the magnetopause mode grows significantly faster than the inner mode [*Lee et al.*, 1981, Figure 2]. For the April 29, 1993, event, the DMSP precipitation data suggested that the IMF was northward for the earlier half of the 1-hour interval 1400–1500 UT (though, more likely southward during the second half) (P. T. Newell, private communication, 1998). Furthermore, the phase velocity of the magnetopause mode can be comparable to the flow speed of the magnetosheath. Thus, the present event is better explained in terms of the magnetopause mode. It should also be noted that many previous studies reported the wavy motion of the magnetopause (section 3.1), which is more favorable for the magnetopause mode than for the inner mode. The role of the K-H instability at the magnetopause might have been understated in the past.

In the actual magnetosphere, the transition from the solar wind to the plasma sheet takes place in a continuous way through the LLBL. Numerical studies of the K-H instability show that for a velocity shear with a finite thickness d, the growth rate is maximum when a wave vector component perpendicular to the magnetic field and parallel to the plasma flow, $k_\perp$, is $1/(2d)$ [*Walker* 1981; *Miura and Pritchett*, 1982; *Rostoker et al.*, 1984]. For the present event, d is estimated at 7000 km (1.1 R_E) from the wavelength, 90,000 km (section 2.3). The estimate is within, but close to the upper limit of, the range of the thickness of the LLBL at the flank of the magnetosphere [*Eastman and Hones*, 1979].

In the present event, the entire morningside magnetosphere oscillated at the single frequency. This is not self-evident from the viewpoint of the K-H instability since the wavelength, and therefore also the frequency, of the most unstable mode depends on the thickness of the velocity shear layer, which is inferred to increase with the distance from the subsolar point [*Eastman and Hones*, 1979]. However, it is expected that spatial structures of a K-H mode coalesce into longer-scale ones as a wave propagates antisunward [*Wu*, 1986; *Wei et al.*, 1990; *Thomas and Winske*, 1993]. Such coalescence possibly explains the x dependence of wave periods (Figure 17) and the thick velocity shear layer inferred above. Inside the magnetosphere, a dominant wave frequency may be determined by an oscillation with the longest longitudinal scale, since such an oscillation should have the longest characteristic (e-folding) length in the radial direction and therefore can reach deeper in the magnetosphere. Numerical simulation with realistic magnetic field configuration and magnetosheath flow distribution is desirable for understanding the spatial development of the K-H instability.

4. Summary

In this paper, we examined the morningside *Pc5* event of April 29, 1993, by using a coordinated data set acquired at different altitudes in the magnetosphere and on the ground. The magnetic field oscillated at the same period, 5 min, at Geotail in the boundary region and at geosynchronous altitude. Furthermore, the ground stations, which are distributed in several hours of local time and in a wide range of latitude from the auroral zone to equatorward of a region 2 current, observed the corresponding oscillations. These results indicate that almost the entire morningside magnetosphere oscillated at the same frequency. From the absence of the 90° phase difference between the magnetic field and electric field variations at Geotail we conclude that the oscillation was continuously excited. We infer that the most plausible excitation mechanism for the present event is the K-H instability at the magnetopause. This idea is consistent with the polarization of the rotation of the plasma flow velocity at Geotail and that of ground magnetic variations, and is also supported by the antisunward propagation of the wave at a velocity comparable to the magnetosheath flow speed.

Acknowledgments. We wish to thank A. Miura for fruitful discussions. We are also grateful to L. Eliasson for the information about the Freja particle signature. Thanks also to D. Holland and S. R. Nylund of JHU/APL for their assistance in processing the Freja magnetic field and Geotail EPIC data, respectively. We also thank H. Kawano and S. Wing for their help for the coordinate transformation of the GOES magnetometers data. PACE coordinate software was provided by K. B. Baker. The Hermanus ground magnetometer data were provided by the World Data Center C2. Work at JHU/APL was supported by NASA, NSF, and the Office of Naval Research.

Janet G. Luhmann thanks Roger Arnoldy and David M. Walker for their assistance in evaluating this paper.

References

Anderson, B. J., An overview of spacecraft observations of 10 s to 600 s period magnetic pulsations in the Earth's magnetosphere, in *Solar Wind Sources of Magnetospheric Ultra-Low Frequency Waves, Geophys. Monogr. Ser.*, vol. 81, edited by M. J. Engebretson, K. Takahashi, and M. Scholer, p. 25, AGU, Washington, D. C., 1994.

Anderson, B. J., M. J. Engebretson, S. P. Rounds, L. J. Zanetti, and T. A. Potemra, A statistical study of *Pc* 3–5 pulsations observed by the AMPTE/CCE magnetic field experiment, 1, Occurrence distributions, *J. Geophys. Res.*, *95*, 10,495, 1990.

Atkinson, G., and T. Watanabe, Surface waves on the magnetospheric boundary as a possible origin of long period geomagnetic micropulsations, *Earth Planet. Sci. Lett.*, *1*, 89, 1966.

Aubry, M. P., M. G. Kivelson, and C. T. Russell, Motion and structure of the magnetopause, *J. Geophys. Res.*, *76*, 1673, 1971.

Baker, K. B., and S. Wing, A new magnetic coordinate system for conjugate studies at high latitude, *J. Geophys. Res.*, *94*, 9139, 1989.

Bendat, J. S., and A. G. Piersol, *Random Data: Analysis and Measurement Procedures*, p. 407, John Wiley, New York, 1971.

Cahill, L. J., Jr., N. G. Lin, M. J. Engebretson, D. R. Weimer, and M. Sugiura, Electric and magnetic observations of the structure of standing waves in the magnetosphere, *J. Geophys. Res.*, *91*, 8895, 1986.

Chen, L., and A. Hasegawa, A theory of long-period magnetic pulsations, 1, Steady state excitation of field line resonance, *J. Geophys. Res.*, 79, 1024, 1974.

Chen, S.-H., and M. G. Kivelson, On nonsinusoidal waves at the Earth's magnetopause, *Geophys. Res. Lett.*, *20*, 2699, 1993.

Chen, S.-H., M. G. Kivelson, J. T. Gosling, R. J. Walker, and A. J. Lazarus, Anomalous aspects of magnetosheath flow and of the shape and oscillations of the magnetopause during an interval of strongly northward interplanetary magnetic field, *J. Geophys. Res.*, *98*, 5727, 1993.

Clauer, C. R., A. J. Ridley, R. J. Sitar, H. J. Singer, A. S. Rodger, E. Friis-Christensen, and V. O. Papitashvili, Field-line resonant pulsations associated with a strong dayside ionospheric shear convection flow reversal, *J. Geophys. Res.*, *102*, 4585, 1997.

Couzens, D., G. K. Parks, K. A. Anderson, R. P. Lin, and H. Reme, ISEE particle observations of surface waves at the magnetopause boundary layer, *J. Geophys. Res.*, *90*, 6343, 1985.

Cummings, W. D., R. J. O'Sullivan, and P. J. Coleman, Jr., Standing Alfvén waves in the magnetosphere, *J. Geophys. Res.*, *74*, 778, 1969.

Eastman, T. E., and E. W. Hones, Jr., Characteristics of the magnetospheric boundary layer and magnetopause layer as observed by IMP 6, *J. Geophys. Res.*, *84*, 2019, 1979.

Eastman, T. E., J. E. W. Hones, S. J. Bame, and J. R. Asbridge, The magnetospheric boundary layer: Site of plasma, momentum, and energy transfer from the magnetosheath into the magnetosphere, *Geophys. Res. Lett.*, *3*, 685, 1976.

Eliasson, L., et al., The Freja hot plasma experiment–Instrument and first results, *Space Sci. Rev.*, *70*, 563, 1994.

Fairfield, D. H., Average and unusual locations of the Earth's magnetopause and bow shock, *J. Geophys. Res.*, *76*, 6700 1971.

Fairfield, D. H., W. Baumjohann, G. Paschmann, H. Lühr, and D. G. Sibeck, Upstream pressure variations associated with the bow shock and their effects on the magnetosphere, *J. Geophys. Res.*, *95*, 3773 1990.

Greenwald, R. A., and A. D. M. Walker, Energetics of long period resonant hydromagnetic waves, *Geophys. Res. Lett.*, *7*, 745, 1980.

Hasegawa, A., *Plasma Instabilities and Nonlinear Effects*, pp. 125–129, Springer-Verlag, New York, 1975.

Hones, E. W., Jr., G. Paschmann, S. J. Bame, J. R. Asbridge, N. Sckopke, and K. Schindler, Vortices in magnetospheric plasma flow, *Geophys. Res. Lett.*, *5*, 2069, 1978.

Kivelson, M. G., and S.-H., Chen, The magnetopause: Surface waves and instabilities and their possible dynamics consequences, in *Physics of the Magnetopause, Geophys. Monogr. Ser.*, vol. 90, edited by P. Song, B. U. Ö. Sonnerup, and M. F. Thomsen, p. 257, AGU, Washington, D. C., 1995.

Kokubun, S., Statistical characteristics of *Pc*5 waves at synchronous orbit, *J. Geomagn. Geoelectr.*, *37*, 759, 1985.

Kokubun, S., R. L. McPherron, and C. T. Russell, OGO 5 observations of *Pc*5 waves: Ground-magnetosphere correlations, *J. Geophys. Res.*, *81*, 5141, 1976.

Kokubun, S., K. N. Erickson, T. A. Fritz, and R. L. McPherron, Local time asymmetry of *Pc* 4-5 pulsations and associated particle modulations at synchronous orbit, *J. Geophys. Res.*, *94*, 6607, 1989.

Kokubun, S., T. Yamamoto, M. H. Acuña, K. Hayashi, K. Shiokawa, and H. Kawano, The Geotail magnetic field experiment, *J. Geomagn. Geoelectr.*, *46*, 7, 1994a.

Kokubun, S., H. Kawano, M. Nakamura, T. Yamamoto, K. Tsuruda, H. Hayakawa, A. Matsuoka, and L. A. Frank, Quasi-periodic oscillations of the magnetopause during northward sheath magnetic field, *Geophys. Res. Lett.*, *21*, 2883, 1994b.

Lee, L. C., R. K. Albano, and J. R. Kan, Kelvin-Helmholtz instability in the magnetopause-boundary layer region, *J. Geophys. Res.*, *86*, 54, 1981.

Lepping, R. P., and L. F. Burlaga, Geomagnetic surface fluctuations observed by Voyager 1, *J. Geophys. Res.*, *84*, 7099, 1979.

Lundin, R., G. Haerendel, and S. Grahn, The Freja science mission, *Space Sci. Rev.*, *70*, 465, 1994.

Mitchell, D. G., M. J. Engebretson, D. J. Williams, C. A. Cattell, and R. Lundin, *Pc*5 pulsations in the outer dawn magnetosphere seen by ISEE 1 and 2, *J. Geophys. Res.*, *95*, 967, 1990.

Miura, A., Kelvin-Helmholtz instability at the magnetospheric boundary: Dependence on the magnetosheath sonic Mach number, *J. Geophys. Res.*, *97*, 10,655, 1992.

Miura, A., and P. L. Pritchett, Nonlocal stability analysis of the MHD Kelvin-Helmholtz instability in a compressible plasma, *J. Geophys. Res.*, *87*, 7431, 1982.

Nakamura, M., H. Matsui, H. Kawano, S. Kokubun, K. Takahashi, A. Matsuoka, T. Yamamoto, K. Tsuruda, H. Hayakawa, and T. Okada, *Pc*5 pulsations observed in the dayside magnetosphere by Geotail, *Geophys. Res. Lett.*, *21*, 2903, 1994.

Ogilvie, K. W., and R. J. Fitzenreiter, The Kelvin-Helmholtz instability at the magnetopause and inner boundary layer surface, *J. Geophys. Res.*, *94*, 15,113, 1989.

Olson, J. V., and G. Rostoker, Longitudinal phase variations of *Pc* 4-5 micropulsations, *J. Geophys. Res.*, *83*, 2481, 1978.

Potemra, T. A., and L. G. Blomberg, A survey of *Pc*5 pulsations in the dayside high latitude regions observed by Viking, *J. Geophys. Res.*, *101*, 24,801, 1996.

Potemra, T. A., H. Lühr, L. J. Zanetti, K. Takahashi, R. E. Erlandson, G. T. Marklund, L. P. Block, L. G. Blomberg, and R. P. Lepping, Multisatellite and ground-based observations of transient ULF waves, *J. Geophys. Res.*, *94*, 2543, 1989.

Roelof, E. C., and D. G. Sibeck, Magnetopause shape as a bivariate function of interplanetary magnetic field B_z and solar wind dynamic pressure, *J. Geophys. Res.*, *98*, 21,421, 1993.

Rostoker, G., I. Spadinger, and J. C. Samson, Local time variation in the response of *Pc*5 pulsations in the morning sector to substorm expansive phase onsets near midnight, *J. Geophys. Res.*, *89*, 6749, 1984.

Rostoker, G., B. Jackel, and R. L. Arnoldy, The relationship of periodic structures in auroral luminosity in the afternoon sector of ULF pulsations, *Geophys. Res. Lett.*, *19*, 613, 1992.

Samson, J. C., Geomagnetic pulsations and plasma waves in the Earth's magnetosphere, in *Geomagnetism*, vol. 4, edited by J. A. Jacobs, p.481, Academic, San Diego, Calif., 1991.

Samson, J. C., J. A. Jacobs, and G. Rostoker, Latitude-dependent characteristics of long-period geomagnetic micropulsations, *J. Geophys. Res.*, *76*, 3675, 1971.

Sarafopoulos, D. V., Simultaneous observation of *Pc*5 pulsations in the dawn and dusk low-latitude boundary layer, *Ann. Geophys.*, *11*, 990, 1993.

Sckopke, N., G. Paschmann, G. Haerendel, B. U. Ö. Sonnerup, S. J. Bame, T. G. Forbes, J. E. W. Hones, Jr., and C. T. Russell, Structure of low-latitude boundary layer, *J. Geophys. Res.*, *86*, 2099, 1981.

Seon, J., L. A. Frank, A. J. Lazarus, and R. P. Lepping, Surface waves on the tailward flanks of the Earth's magnetopause, *J. Geophys. Res.*, *100*, 11,907, 1995.

Sibeck, D. G., et al., The magnetospheric response to 8-minute period strong-amplitude upstream pressure variations, *J. Geophys. Res.*, *94*, 2505, 1989.

Singer, H. J., and M. G. Kivelson, The latitudinal structure of *Pc*5 waves in space: Magnetic and electric field observations, *J. Geophys. Res.*, *84*, 7213, 1979.

Singer, H. J., W. J. Hughes, and C. T. Russell, Standing hydromagnetic waves observed by ISEE 1 and 2: Radial extent and harmonic, *J. Geophys. Res.*, *87*, 3519, 1982.

Song, P., R. C. Elphic, and C. T. Russell, ISEE 1 and 2 observations of the oscillating magnetopause, *Geophys. Res. Lett.*, *15*, 744, 1988.

Southwood, D. J., Some features of field line resonances in the magnetosphere, *Planet. Space Sci.*, *22*, 483, 1974.

Takahashi, K., and R. L. McPherron, Harmonic structure of *Pc*3-4 pulsations, *J. Geophys. Res.*, *87*, 1504, 1982.

Takahashi, K., and R. L. McPherron, Standing hydromagnetic oscillations in the magnetosphere, *Planet. Space Sci.*, *32*, 1343, 1984.

Takahashi, K., R. L. McPherron, and W. J. Hughes, Multispacecraft observations of the harmonic structure of *Pc*3-4 magnetic pulsations, *J. Geophys. Res.*, *89*, 6758, 1984.

Takahashi, K., D. G. Sibeck, P. T. Newell, and H. E. Spence, ULF waves in the low-latitude boundary layer and their relationship to magnetospheric pulsations: A multisatellite observation, *J. Geophys. Res.*, *96*, 9503, 1991.

Tamao, T., Transmission and coupling resonance of hydromagnetic disturbances in the non-uniform Earth's magnetosphere, *Sci. Rep. Tohoku Univ., Ser. 5, 17*, 43, 1966.

Thomas, V. A., and D. Winske, Kinetic simulations of the Kelvin-Helmholtz instability at the magnetopause, *J. Geophys. Res.*, *98*, 11,425, 1993.

Traver, D. P., D. G. Mitchell, D. J. Williams, L. A. Frank, and C. Y. Huang, Two encounters with the frank low-latitude boundary layer: Further evidence for closed field topology and investigation of the internal structure, *J. Geophys. Res.*, *96*, 21,025, 1991.

Tsuruda, K., H. Hayakawa, M. Nakamura, T. Okada, A. Matsuoka, F. S. Mozer, and R. Schmidt, Electric field measurements on the Geotail satellite, *J. Geomagn. Geoelectr.*, *46*, 693, 1994.

Walker, A. D. M., The Kelvin-Helmholtz instability in the low-latitude boundary layer, *Planet. Space Sci.*, *38*, 213, 1981.

Waters, C. L., J. C. Samson, and E. F. Donovan, The temporal variation of the frequency of high-latitude field line resonances, *J. Geophys. Res.*, *100*, 7987, 1995.

Wei, C. Q., L. C. Lee, and A. L. L. Belle-Hamer, A simulation study of the vortex structure in the low-latitude boundary layer, *J. Geophys. Res.*, *95*, 20,793, 1990.

Williams, D. J., D. G. Mitchell, T. E. Eastman, and L. A. Frank, Energetic particle observations in the low-latitude boundary layer, *J. Geophys. Res.*, *90*, 5097, 1985.

Williams, D. J., R. W. McEntire, C. Schlemm II, A. T. Y. Lui, G. Gloeckler, S. P. Christon, and F. Gliem, Geotail energetic particles and ion composition instrument, *J. Geomagn. Geoelectr.*, *46*, 39, 1994.

Winningham, J. D., F. Yasuhara, S.-I. Akasofu, and W. J. Heikkila, The latitudinal morphology of 10-eV to 10-keV electron fluxes during magnetically quiet and disturbed times in the 2100–0300 MLT sector, *J. Geophys. Res.*, *80*, 3148, 1975.

Wolfe, A., L. J. Lanzerotti, and C. G. Maclennan, Dependence of hydromagnetic energy spectra on solar wind velocity and interplanetary magnetic field direction, *J. Geophys. Res.*, *85*, 114, 1980.

Wu, C. C., Kelvin-Helmholtz instability at the magnetopause boundary, *J. Geophys. Res.*, *91*, 3042, 1986.

Zanetti, L. J., et al., Magnetic field experiment for the Freja satellite, *Space Sci. Rev.*, *70*, 465, 1994.

Ziesolleck, C. W. S., and D. R. McDiarmid, Auroral latitude Pc5 field line resonances: Quantized frequencies, spatial characteristics, and diurnal variation, *J. Geophys. Res.*, *99*, 5817, 1994.

V. Angelopoulso, Space Science Laboratory, University of California, Berkeley, CA 94720. (e-mail: vassilis@ssl.berkeley.edu)

J. B. Gary, A. T. Y. Lui, S. Ohtani, D. J. Williams, and L. J. Zanetti, The Johns Hopkins University Applied Physics Laboratory, 11100 Johns Hopkins Road, Laurel, MD 20723. (e-mail: GARYJB1@aplmail.jhuapl.edu; LUIAT1@jhuapl.edu; ohtani@fluxgate.jhuapl.edu; WILLIDJ1@jhuaapl.edu; ZANETLJ1@jhuapl.edu)

W. J. Hughes, Department of Astronomy, Boston University, Boston, MA 02215. (e-mail: hughes@buasta.bu.edu)

S. Kokubun and K. Takahashi, Solar-Terrestrial Environment Laboratory, Nagoya University, Toyokawa 442, Japan. (e-mail: kokubun@stelab.nagoya-u.ac.jp; kazue.takahashi@jhuapl.edu)

M. Nakamaura, Department of Earth and Planetary Physics, University of Tokyo, Tokyo 113, Japan. (e-mail: mnakamur@grl.s.u-tokyo.ac.jp)

G. Rostoker, Department of Physics, University of Alberta, Edmonton, Alberta, Canada ABT6G21. (e-mail:rostoker@space.ualberta.ca)

H. Singer, NOAA R/E/SE, Boulder, CO 80303. (e-mail:hsinger@sec.noaa.gov)

K. Tsuruda, Institute of Space and Astronautical Science, Sagamihara 229, Japan. (e-mail: tsuruda@gtl.isas.ac.jp)

C. Waters, Department of Physics, University of New Castle, Callaghan, NSW 2308, Australia. (e-mail: physpuls8@cc.newcastle.edu.au)

(Received May 15, 1998; revised September 8, 1998; accepted September 16, 1998.)